Highlights of Spanish Astrophysics XII, Proceedings of the XVI Scientific Meeting of the Spanish Astronomical Society held on July 15 - 19, 2024, in Granada, Spain. M. Manteiga, F. González Galindo, A. Labiano Ortega, M. Martínez González, N. Rea, M. Romero Gómez, A. Ulla Miguel, G. Yepes, C. Rodríguez López, A. Gómez García and C. Dafonte (eds.), 2025

Galaxies in the CATARSIS clusters: study of the properties and reconstruction of the SFHs from their SED modeling

Macías-Pardo, P.[1,2]**, Gil de Paz, A.**[1,2]**, Catalán-Torrecilla, C.**[1,2]**, Castillo-Morales, Á.**[1,2]**, Sánchez-Blázquez, P.**[1,2]**, Callejas-Córdoba, B.**[1,2]**, TARSIS Consortium and instrument team, and CATARSIS team**

[1] Departamento de Física de la Tierra y Astrofísica, Fac. CC. Físicas, Universidad Complutense de Madrid, Plaza de las Ciencias, 1, Madrid, E-28040, Spain
[2] Instituto de Física de Partículas y del Cosmos, IPARCOS-UCM, Fac. CC. Físicas, Universidad Complutense de Madrid, Plaza de las Ciencias 1, Madrid, E-28040, Spain

Abstract

CATARSIS will survey 16 galaxy clusters in the redshift range $0.15 \leq z \leq 0.23$ to understand the formation of structures and the evolution of galaxies in their dynamic and growing environment using TARSIS ("Tetra-Armed Super-Ifu spectrograph"), the future wide-field ($\sim$ 8 arcmin^2) Integral Field Spectrograph to be installed at the CAHA 3.5m telescope in 2028, with spectral coverage 320-810 nm and resolving power R $\sim$ 1000. We are collecting deep multi-wavelength optical and near-infrared (nIR) imaging from existing surveys (SDSS, LS, GALEX, 2MASS, WISE, Euclid) in addition to deep u-band and JHK_s data from in progress long-term programs by using telescopes at CAHA to complement and extend the TARSIS wavelength range. All this to build and model the spectral energy distributions (SEDs) of cluster galaxies, as well as to constrain their star formation history (SFH) and star formation rate (SFR).

1 Introduction

Galaxy clusters are the largest gravitationally bound structures in the Universe. Their masses, gravitational potentials, and spatial distributions are closely linked to the growth of cosmic structure and the Universe's formation history. Determining the mass distribution in galaxy clusters provides essential information about cosmological parameters and the nature of dark matter. It also enables tests of gravity theories and helps to study the environmental processes influencing galaxy evolution and the intergalactic medium ([12], [13], [8]). In this context, the CATARSIS project was developed to enable the precise determination of mass profiles. CATARSIS is the new legacy survey for the 3.5m telescope at the Calar Alto Observatory. Over the course of 600 dark nights, it will observe a sample of 16 galaxy clusters at redshifts z $\sim 0.15 - 0.23$ using the new TARSIS instrument (Tetra-ARmed-Super-IFU-Spectrograph), which has an 8,arcmin$^{\mathbf{2}}$ field of view. The survey will map all objects within the clusters' virial radii, as well as foreground and background galaxies. One of its main goals is to estimate the mass profiles by applying the Caustic technique [6]. This method models the positions and radial velocities of cluster members as projections of their 3D phase-space distribution. For the first time, the survey will use an unbiased spectroscopic sample of cluster galaxies. This is especially useful in cluster outskirts, where red-sequence galaxies, commonly targeted by other surveys, are less dominant and contaminants are more numerous.

The survey has several overarching goals. These include studying the substructure of CATARSIS clusters, analyzing the intrinsic alignment of galaxies' angular momentum with filaments, and quantifying residual star formation in cluster galaxies. The survey will also investigate the galaxies' star formation histories (SFHs) as a function of their properties. Achieving these objectives requires precise spectrophotometric calibration, detailed analysis of disk galaxy spiral morphologies, and measurements of sizes, ellipticities, and position angles. These parameters are critical for complementary lensing mass-profile determinations ([4]). Additionally, the survey aims to recover very low levels of residual star formation and compare them with those observed in cluster periphery galaxies. High-quality, deep imaging data are crucial for these studies. While some surveys provide gri imaging with sufficient depth and spatial resolution, two important spectral gaps remain: the u-band (significantly overlapping with the TARSIS blue range) and the near-infrared (nIR). To address this, a long-term program is underway using CAHA telescopes. This program includes u-band imaging with CAFOS@2.2m and JHK_s nIR imaging with Omega2000@3.5m, extending coverage of CATARSIS clusters well beyond their virial radii.

2 Scientific preparation of CATARSIS: status of the observations

Each of the 16 CATARSIS clusters will be observed by four pointings (p1–p4) that cover regions within the cluster's virial radius. When the cluster's shock radius extends beyond the p1–p4 field of view, we complement these observations with eight additional pointings (o1–o8) around the outskirts of the cluster. Each pointing will comprise two hours of observational time. The program spans seven semesters, beginning in autumn 2023 and potentially extending into 2027. Observing the shock radius is particularly important for studying recent star formation beyond the cluster's boundaries. These outer regions will only be imaged in the CAFOS u-band. Near-infrared (nIR) imaging, on the other hand, will play a crucial role in providing structural information that is less affected by dust attenuation or recent star formation. It will also enhance the contrast of spiral arms. As demonstrated in [7], adding $JHKs$ photometry to optical SEDs is essential for deriving accurate stellar masses and mass-weighted ages.

Table 1: Status of the CAFOS and Omega2000 observations

Cluster ID	u-band CAFOS	J O2000	H O2000	Ks O2000
CTRS01	c1, p1, p3, p4	p1, p2, p3	p1, p2	p1, p2, p3
CTRS02				
CTRS03	c1			
CTRS06	c1	p1, p2	p1, p2	p1
CTRS08	c1			
CTRS09	c1			
CTRS14				
CTRS18	c1, p1			
CTRS19	c1, p1			
CTRS24	c1			
CTRS25	c1			
CTRS27	c1, p1, p2, p3			
CTRS29	c1			
CTRS31	c1, p1	p1, p2, p3	p1, p2, p3	p1, p2, p3
CTRS32	p1	p1	p1	
CTRS33				

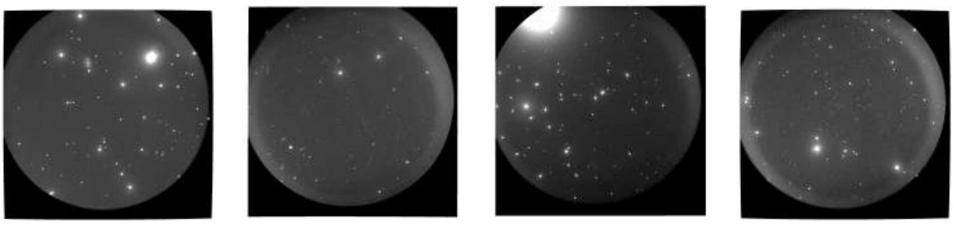

Figure 1: Reduced and combined central pointing (c1) images for the clusters CTRS01, CTRS18, CTRS19, and CTRS27 (from left to right).

The u-band data reduction was performed using the FILABRES software package [2], developed for the automatic reduction of direct images obtained with the CAFOS instrument. The workflow of FILABRES begins with image classification (e.g., bias, flat-field, and science images), followed by the reduction of calibration images, the creation of combined master calibrations, and, finally, the reduction of individual science images. In some cases, the appearance of an illumination pattern necessitated the use of super-flats. Astrometric calibration was performed using tools from Astrometry [11] and Astromatic[1]. Images from the individual pointings (p1–p4) within a cluster were co-aligned and combined to create a preliminary image for that night, and then merged into a final mosaic covering the cluster. Figure 1 presents examples of central pointings for clusters CTRS01, CTRS18, CTRS19, and CTRS27. Table 1 collects the status of observations with CAFOS and Omega2000.

[1]https://github.com/astromatic

3 Construction of catalogs for SED fitting

We use available data from existing large surveys such as the Sloan Digital Sky Survey (SDSS) DR18 and the Legacy Survey (LS) DR10, together with the Wide-Field Infrared Explorer (WISE) to model their SEDs and derive their main physical quantities as a first step to conduct the scientific preparation of the CATARSIS clusters. To combine data from catalogs, we applied corrections and selected models to ensure consistency across datasets. Galactic extinction corrections are applied based on values provided by LS. The LS photometric catalogs offer morphological classifications in r-band fluxes, including PSF, exponential, round-exponential, de Vaucouleurs, and Sérsic profiles. In contrast, SDSS catalogs provide these model fluxes directly (except for the Sérsic type), along with the best-fit model between exponential and de Vaucouleurs in each band or a composite flux from these two models. We decided to use the morphological model given by LS in the r-band and extend it to the other bands, except for the Sérsic type, for which we used aperture fluxes for SDSS data. In the case of exponential and de Vaucouleurs models, we first compared inverse variances in the r-band to confirm the selection within SDSS data.

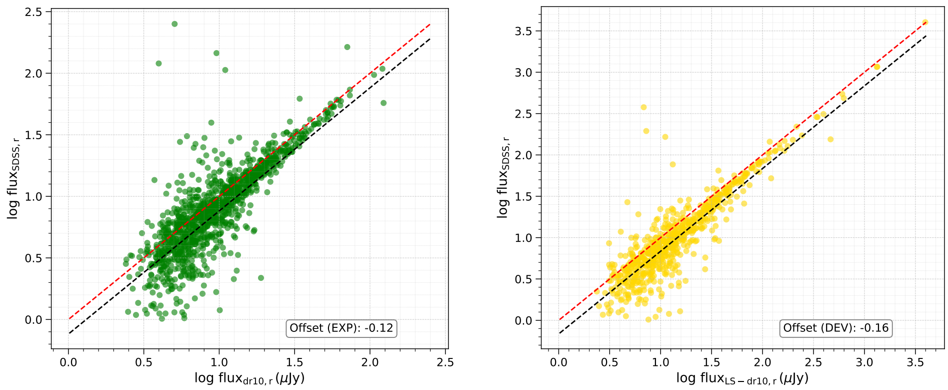

Figure 2: Offsets derived between SDSS-DR18 and LS-DR10 catalogs based on the model flux types provided by LS for exponential and de Vaucouleurs models.

The final input photometry used to model the SEDs is based on SDSS $ugriz$ band fluxes selected according to these criteria. For LS fluxes, we use the dereddened r-band fluxes with the offsets derived (two examples are shown in Fig. 2), and for the remaining g, i, and z bands, the final fluxes required for the SED fitting are obtained from their catalog colors. Additionally, dereddened WISE fluxes are incorporated. The SED fitting is conducted with the Python code Bagpipes (Bayesian Analysis of Galaxies for Physical Inference and Parameter Estimation; [3]), a tool for modeling galaxy spectra and fitting both spectroscopic and photometric observations. Bagpipes generates model galaxy spectra spanning from the far-ultraviolet to the mm-wavelengths regime and fits these models to arbitrary combinations of photometric and spectroscopic observational data using MULTINEST (multimodal nested sampling algorithm [5]). Models are constructed by specifying key parameters for different components, including dust, nebular emission, and SFH. While Bagpipes does not implement stellar population synthesis (SPS) directly, it operates with predefined SPS models in the form of grids of simple stellar population (SSP) models across a range of ages and metallicities. The SPS models used are the 2016 version of Bruzual & Charlot [1], with a Kroupa & Boily initial mass function (IMF) [10].

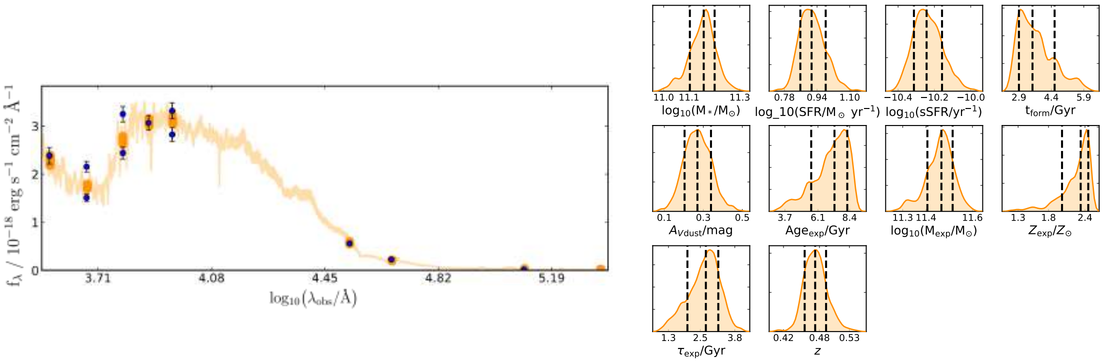

Figure 3: Example from the SED fitting using Bagpipes along with the posterior distributions of derived quantities.

We aim to develop cluster membership criteria and derive their physical properties from the fittings. As a preliminary step, we performed SED fitting on photometric data to obtain the posterior distribution for physical quantities such as SFR, mass-weighted age, stellar mass, redshift, and others, illustrated in Fig. 3. Among these quantities, we are particularly interested in the determination of redshift to define cluster members. In the end, this redshift is treated as a fixed parameter in the SFH model component to the subsequent determination of posterior quantities, thereby avoiding possible degeneracies. To achieve this, we use a subsample of galaxies in each cluster that already have spectroscopic redshifts and perform the fittings in two steps, considering large deviations from the fit in the u-band flux and between catalogs for the grz fluxes in the second step.

We compare the spectroscopic redshifts and determine a confidence interval around the cluster redshift to optimize the false positive rate, sensitivity (true positives) and specificity (true negatives). For cluster CTRS32, Fig. 4 shows an accumulation of redshifts in the interval $[0.2, 0.4]$, indicating that our fittings tend to overestimate the redshifts. From the color-magnitude plot, we use the red sequence to apply an additional color limit and remove (redder) background contaminants. The red sequence used is obtained from the slope provided by [9] for the redshift of the cluster and the intercept from the median $g - r$ color. Table 2 presents the results for cluster CTRS32 after removing galaxies significantly redder than the red sequence (RS), which reduces the number of false positives.

Acknowledgments

This research has been funded by the spanish Agencia Estatal de Investigación (AEI) and Ministerio de Ciencia e Innovación (MCIN) under the projects PID2022-138621NB-I00, PID2022-138855NB-C31 and PID2021-123417OB-I00. Authors also acknowledge the finantial support from the program

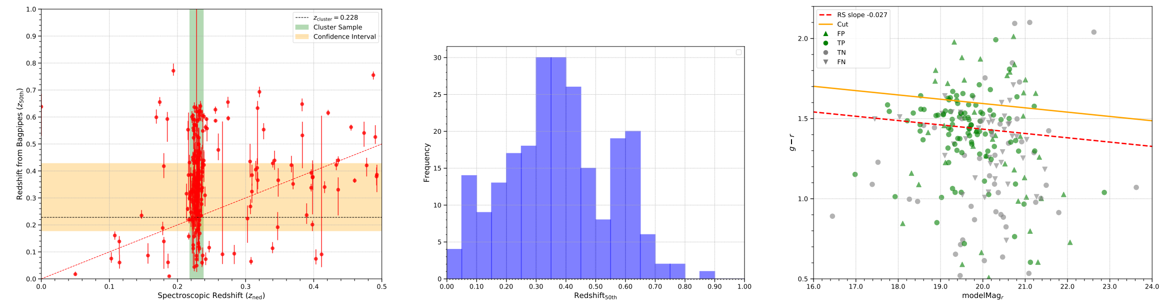

Figure 4: Results from the redshift determination using Bagpipes for cluster CTRS32 (Abell 2390): comparison with the spectroscopic redshift in a selected confidence interval (left), histogram of the median posterior probability distribution of redshift (center), and color-magnitude diagram for the galaxies in cluster CTRS32, classified according to the confidence interval around the cluster redshift ($z = 0.228$)

Table 2: Results for the cluster membership criterion

	Confidence interval	RS cut
FPR	0.479	0.270
Sensitivity	0.700	0.649
Specificity	0.525	0.720

Tecnologías Avanzadas para la Exploración del Universo y sus Componentes (TAU-CM).

References

[1] Bruzual G., Charlot S., 2003, MNRAS, 344, 1000 (BC03)

[2] Cardiel N. et al., 2020, SMSAS, 219

[3] Carnall, A. C., McLure, R. J., Dunlop, J. S. & Davé, R., 2018, MNRAS, 480, 4

[4] Diaferio A., Geller M.J. & Rines, K. J., 2005, ApJ, 628, L97

[5] Feroz F. & Hobson M. P., 2008, MNRAS, 384, 2

[6] Gifford, D., Miller, C. & Kern, N., 2013, ApJ, 773, 116

[7] Gil de Paz, A., & Madore, B., 2002, AJ 123, 1864

[8] Gladders, M. D. et al., 2007, ApJ, 655, 128

[9] Hao, Jiangang et al, 2009, ApJ, 702, 745

[10] Kroupa P. & Boily C. M., 2002, MNRAS, 336, 1188

[11] Lang, D., Hogg, D. W., Mierle, K., Blanton, M. & Roweis S., 2010, AJ, 139, 1782

[12] Milgrom, M., 2002, ApJ, 577, L75

[13] McGaugh, S., 2015, Can. J. Phys., 93, 250